J. Eng. Technol. Sci., Vol. 53, No. 2, 2021, 210204

Study of the Evaporation Process in the Spray Zone of a Mechanical Draft Wet Cooling Tower

Dany Iman Santoso[1]*, Bambang Antoko[2], Prabowo[3] & Djatmiko Ichsani[3]

[1]Department of Mechanical Engineering, Universitas Negeri Surabaya
Jalan Ketintang, Surabaya 60231, Indonesia
[2]Department of Mechanical Engineering, Politeknik Perkapalan Negeri Surabaya
Jalan Teknik Kimia, Surabaya 60111, Indonesia
[3]Department of Mechanical Engineering, Institut Teknologi Sepuluh Nopember
Jalan Teknik Industri, Surabaya 60111, Indonesia
*E-mail: danysantoso@unesa.ac.id

Highlights:

- Droplet radius and radius evolution graphs.
- Droplet mass and its rate graphs.
- Droplet temperature and its rate graphs.

Abstract. The evaporation process in the nozzle spray system of a cooling tower was the main object of study in order to determine its performance. This process involves liquid water in small size, usually at the droplet level. At this level, parameters that affect the droplet size, such as capacity, air velocity in the chamber, water pressure at the nozzle, atmospheric temperature, etc., influence the process of heat and mass transfer. In this study, capacity and fan rotation were varied to obtain a graph showing the evaporation. Radius, velocity, mass and temperature graphs and rate graphs were obtained from mathematical modeling of the governing equations. From the results it appears that evaporation occurs at a capacity of 6 liter per minute and above, but this requires further proof of the evaporation process along with the height of the tower, which will be the subject of a future study.

Keywords: *evaporation process; nozzle spray; cooling tower; droplet level; heat and mass transfer.*

1 Introduction

A cooling tower is a heat exchanger that has high effectiveness [1]; therefore it is widely used in industry and power plants [2]. One type of cooling tower is the natural draft wet cooling tower (NDWCT), which is commonly used in power plants because of its large capacity [3]. Power plants are usually built on the seafront, so salt contained in the cooling water often soils the fill zone and causes a decrease in cooling tower performance [4]. NDWCTs are also called usual

Received March 24th, 2020, Revised July 12th, 2020, Accepted for publication November 19th, 2020
 ISSN: 2337-5779,
DOI: 10.5614/j.eng.technol.sci.2021.53.2.4

NDWCTs (UNDWCTs) to distinguish them from high-level water collecting NDWCTs (HNDWCTs), which have higher efficiency than UNDWCTs [5]. HNDWCTs have high-water collecting devices (HWCDs) positioned higher than the water basin of an UNDWCT [6] so that the power used by the pump is lower [7].

Cooling towers with lower capacity than NDWCTs are mechanical draft wet cooling towers (MDWCTs), which are usually used in medium scale industries, with heights varying from 2 to 12 m [8]. Both NDWCTs and MDWCTs consume large amounts of water for circulation. Another type is the dry cooling system, which uses air-cooled heat exchangers (ACHE). Thus, they do not use water as a working fluid and have lower operating costs [9]. Better knowledge about the evaporation process in cooling towers is important for innovations that could improve their efficiency [10]. One of the factors that influence the evaporation process is the spraying process in the nozzle system.

In the spraying process, the water is at the droplet level, where the acting forces depend on the size of the droplets. Droplet measurements are carried out with prediction theories or image capture using a high-resolution camera. In fact, there are cameras that can photograph not only the size of the droplets [11] but also the temperature distribution inside the droplets [12-14]. To avoid high costs in developing cooling towers, mathematical modeling is done to observe the influential parameters. In this work, an MDWCT prototype (as shown in Figure 1) was used to measure the thermodynamic properties of the working fluid. Then, mathematical modeling was developed to show the rate of change of the parameters at the droplet level, so that the effects of each parameter in the evaporation process could be revealed.

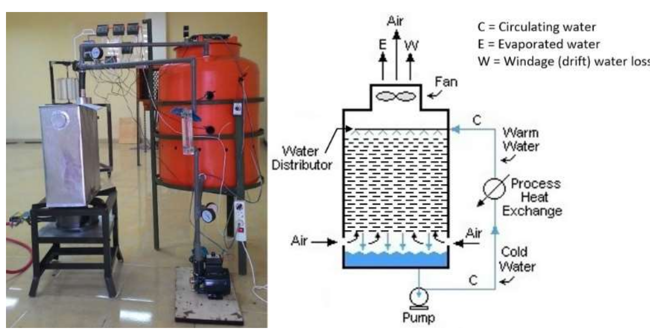

Figure 1 Experimental setup and apparatus.

The four main components in this experiment were a water tank acting as a cooling tower, a water pump, a heat exchanger, and an exhaust fan. A valve was installed before the water pump to control the water flow and a flow meter was installed after it. A water pressure gauge and a thermostat were installed before and after each of the main components. Also, two thermostats were installed inside the cooling tower at different heights to measure the temperature at two different points.

2 Methods

To analyze the droplet problem, the droplet diameter was predicted first and then governing equations were developed to calculate the remaining parameters, i.e. velocity, mass, energy, and its rate. The prediction used the volume approach, because it provides a more accurate value than the mass approach.

2.1 Diameter Prediction and Velocity Calculation

As shown in Figure 1, in a cooling tower water is carried out by air as evaporated water or windage loss. Of course we want water that is carried out as evaporated water, which means that evaporation occurs during the spraying process. However, sometimes water is carried out as windage loss. We need to know the detailed parameters that determine when evaporation or windage occurs.

In chemical kinetic schemes there are diffusion and reaction processes that affect the reaction rate. Diffusion is the 'meeting' of reactant particles until they reach an equilibrium state and the reaction process occurs. The separator of these two processes is the equilibrium state. From this statement we can conclude that windage occurs when the diffusion process is in progress while evaporation occurs when the reaction process is in progress.

Some theories that predict the droplet diameter are the maximum entropy principle (MEP), which produces the mass mean diameter, d_{30} [15]; the same volume-to-surface area ratio, which produces the Sauter mean diameter, d_{32} [16]; and spraying processes that produce the volume mean diameter, d_{50} [11]. Between the mass and the volume, the volume has a closer relationship to the diameter than the mass, because the mass depends on the density to get the diameter while the density itself depends on the temperature, whereas the volume is directly related to the diameter and does not depend on other variables.

In the spraying process, water exits the nozzle in the form of a sheet. The surface of the water sheet meets the air, which causes friction. This friction turns into a wave, which causes modulation of the sheet's thickness. This modulation makes the sheet very thin and breaks it into fragments of Squire wavelength size [11]. By contraction these fragments then break into droplets.

The relationship between droplet size and the spray parameter is estimated with the following two dimensionless numbers [11]:

$$\alpha = \rho_a/\rho_l \text{ and } We = \rho_l u_d^2 b/\sigma \tag{1}$$

where α is the density ratio between air ρ_a and liquid water ρ_l, We is the Weber number, σ is the water surface tension, u_d is the droplet velocity, where $u_d = Q_l/A_n$, Q_l is the capacity of the water, A_n is the nozzle cross-section area, and b is the characteristic length since $b^2 \sim A_n$. By the correlation between the volume median diameter and the Weber number, as proposed by Kooij, *et al.* [11], the formula for droplet diameter d is:

$$d = Cb\alpha^{-1/6}We^{-1/3} \tag{2}$$

where C is the slope of the We graphs to the length of ligaments l with a value of 1.95.

To calculate the diameter growth, the critical radius theory [17] is needed to represent the phase transition of all non-equilibrium models. During the phase transition, the process of nucleation and supercritical droplet growth occurs to rebuild the equilibrium. 'Supercritical' means larger than critical and critical radius r^* corresponds to surface tension σ and supersaturation S, where $S = p_v/p_s$ is the ratio of vapor pressure p_v to saturation pressure p_s. Thus:

$$r^* = \frac{2\sigma}{\rho_d R T_v \ln S} \tag{3}$$

where ρ_d is the droplet density, which is equal to liquid water density ρ_l, R is the specific gas constant, and T_v is the vapor temperature.

The droplet diameter growth is affected by the transfer of heat between the droplet and the surrounding vapor, which has been generalized for a wide range of droplet sizes. The theory [17] is adjusted to the measurement of spray at low pressure. The equation is:

$$\frac{dr}{dt} = \frac{k_v\left(1-\frac{r^*}{r}\right)(T_s-T_v)}{\rho_d h_{fg} r\left(1+3.78\frac{\mathrm{Kn}}{\mathrm{Pr}_v}(1-\psi)\right)} \tag{4}$$

where k_v is the thermal conductivity of the vapor, r is the droplet radius, T_s is the saturation temperature, h_{fg} is the specific enthalpy of evaporation, Kn is the Knudsen number, Pr_v is the vapor Prandtl number, and ψ is the empirical tuning factor. This factor was obtained from the measurement of microphysical cloud simulations projecting the mass distribution function. This has been proposed by Onishi [18], where $\psi = \log_{10} r$.

The average air velocity u_a, which can be obtained from the continuity [19], is:

$$u_a = Q_a/(\rho_a L^2) \tag{5}$$

where Q_a is the air capacity, which depends on fan rotation n and air density ρ_a, and L is the bottom side diameter. From Newton's law of momentum and by defining the droplet relaxation time, $\tau_d = \rho_l d^2/(18\mu_a)$ [20], as well as the Reynold number, $\mathrm{Re}_d = |u_d - u_a| d_d/v_d$ [21], the acceleration is obtained as follows:

$$\frac{du_d}{dt} = \frac{(u_a - u_d)\left(1 + 0.15\mathrm{Re}_d^{0.687}\right)}{\tau_d} \tag{6}$$

where μ_a is the dynamic viscosity of the air and v_d is the kinematic viscosity of the droplets.

2.2 Mass and Energy Conservations

The droplet evaporation process in a cooling tower is an example of a two-phase framework, where each phase is analyzed using the Euler-Lagrange equation. The Euler method models the continuous phase completely, while the Lagrange method allows tracking particle parameters such as trajectory, mass, temperature and phase change [22]. Especially for the phase change there is an interaction between the continuous and discrete phases forming the conservation equations. From these, the mass evolution equation can be derived from the mass equation as follows:

$$\frac{dm_d}{dt} = -\frac{\pi d k_v \mathrm{Nu} \ln(1 + \mathrm{B_M})}{c_{pv}} \tag{7}$$

where k_v is the thermal conductivity of the vapor phase, c_{pv} is the heat capacity of the vapor, and $\mathrm{B_M}$ is the Spalding mass number [23], and Nu is the Nusselt number from the correlation [24]:

$$\mathrm{Nu} = 2\left(1 + 0.3\mathrm{Re}_d^{0.5}\mathrm{Pr}_v^{0.33}\right) \cdot F \tag{8}$$

The Frossling correction, F, and the Spalding mass number, $\mathrm{B_M}$, [25] are given by Eqs. (9) and (10), respectively:

$$F = \frac{1}{\mathrm{B_M}} \ln(1 + \mathrm{B_M}) \tag{9}$$

$$\mathrm{B_M} = \frac{y_{f,s} - y_{f,b}}{1 - y_{f,s}} \tag{10}$$

$y_{f,s}$ is the vapor mass fraction at the droplet surface and $y_{f,b}$ is the vapor mass fraction in the surrounding gas, where $y_{f,s}$ is far smaller than 1 during non-equilibrium evaporation [26].

The process of heat transfer between a droplet and its surroundings occurs through conduction, convection and radiation, however, the last can be ignored because it has a very small value [27]. Thus, the most considered in the process are convection and evaporation, so the energy balance equation is illustrated by the following heat dissipation rate equation:

$$m_d c_{pv} \frac{dT_d}{dt} = h_{fg} \frac{dm_d}{dt} + hA_d(T_d - T_a) \tag{11}$$

where m_d is the droplet mass flow rate, i.e. $m_d = Q_l \times \rho_l$, T_d is the droplet temperature, A_d is the droplet surface area, T_a is the air temperature, and h is the droplet coefficient of the heat transfer.

Finally, the cooling tower performance [4] is described as thermal efficiency:

$$\eta_{th} = \frac{(T_{d,in} - T_{d,m,i})100}{T_{d,in} - T_{wb,in}} \tag{12}$$

where $$T_{d,m,i} = \frac{\sum_i m_{d,i} T_{d,i}}{\sum_i m_{d,i}} \tag{13}$$

$T_{d,in}$ is the temperature of the droplet when it enters the chamber, $T_{d,m,i}$ is the mean droplet temperature from droplet temperature $T_{d,i}$, the droplet mass $m_{d,i}$ of the i-th drop, and $T_{wb,in}$ is the temperature of the wet bulb, obtained from a room thermometer.

3 Results and Discussion

Table 1 shows the MDWCT parameters used in the experiment. The water capacity was varied from 0.5 to 18 Lpm and the fan rotation was varied at 300, 500, 700, 1000, and 1500 rpm.

Table 1 Summary of MDWCT parameters.

Bottom diameter (L)	Fan diameter (d_f)	Nozzle diameter (d_n)	Tower height (H)	Window height (h)	Water capacity (Q_l)	Fan rotation (n)
65 cm	8 in	1 mm	75 cm	20 cm	Max. 18 Lpm	Max. 1500 rpm

The results for the droplet diameter and velocity of the droplets and their respective rates are shown in Figure 2; all of them are presented in logarithmic form. Especially in Figure 2(a), the slope of the rate graph is negative, however, it is described as the negation. As can be seen in Figure 2, the radius has intersecting graphs, while the velocity has parallel graphs. Based on this, the droplet velocity is not entirely affected by air counterflow, because at all spray capacities it has a positive acceleration, which means that the impact of gravity dominates the movement. However, at a small capacity, the ratio between the radius and its evolution is very large, which implies that diffusion is taking place between the droplets and the air. Meanwhile, at a large capacity the ratio becomes smaller because of a greater pressure drop on the sprinklers. Therefore, it can be said that evaporation occurs in this state. Note that the distinguishing point between these processes is the intersection point of the graph, i.e. the equilibrium state.

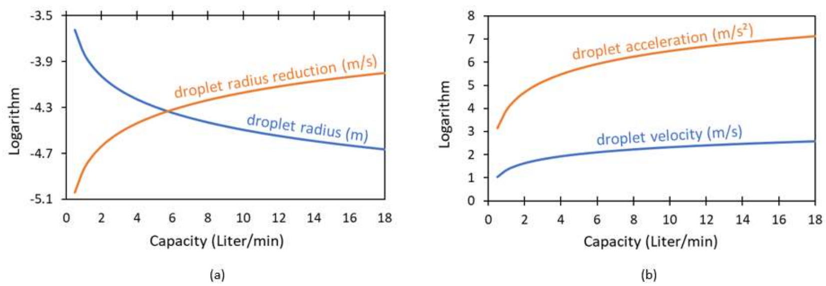

Figure 2 (a) Droplet radius and radius evolution graphs; (b) droplet velocity and acceleration graphs.

The mass and energy conservation equation gives the results shown in Figure 3. The graphs in Figures 3(a) and (b) both have parallel shapes. From Figure 3(a), the ratio between mass and its rate tends to remain constant as long as the capacity varies. This implies that the windage process, or mass transfer, is not visible during variations in capacity because these equations only apply at the nozzle exit. Meanwhile, the mass transfer can only be tracked after the droplet moves along its trajectory.

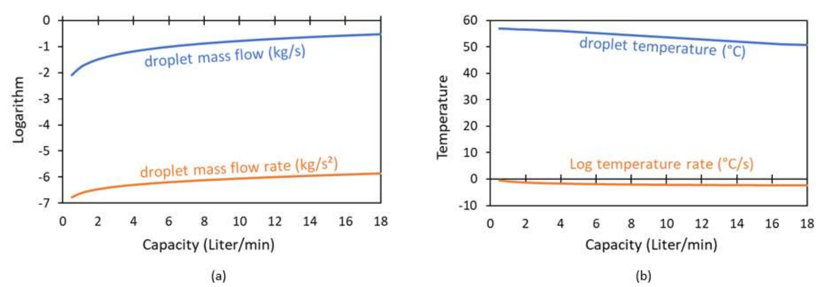

Figure 3 (a) Droplet mass and its rate graphs; (b) droplet temperature and its rate graphs.

On the other hand, as can be seen in Figure 3(b), the evaporation process is clearly visible from the temperature rate. With increasing capacity, temperature differences tend to be constant. This is in accordance with the principle of phase change, which states that during a phase change, temperature and pressure are constant.

Correspondingly, the temperature graph also shows a decrease, which means that the condensation process is going well because of the evaporation process. The existence of the evaporation process is shown in the following graph.

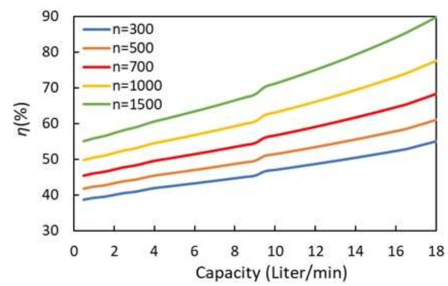

Figure 4 Thermal efficiency graph based on variation of fan rotation.

From Figure 4 it can be stated that the largest capacity combined with the highest fan rotation will produce the greatest efficiency. However, a 100% performance value is impossible because the temperature of the water during water collection cannot be the same as the temperature of the air entering the chamber. The ambient temperature is the boundary of this value.

4 Conclusions

The droplet radius depends on its capacity: the greater the capacity, the smaller the radius. By varying it, we can know the windage process (mass transfer) and the evaporation process (heat transfer). The latter can be tracked clearly in the droplet temperature rate graph, which tends to be constant, while the first needs to track the droplet's trajectory along with the tower height. The point of equilibrium between these processes is at a capacity of 6 Lpm.

The ratio of mass flow rate to mass flow at low capacity is larger than at high capacity. Meanwhile, the temperature rate at high capacity looks more constant than at low capacity. These two things reveal the processes of windage and evaporation at low capacity and high capacity, respectively, in the spray zone of a mechanical draft wet cooling tower.

A future study will focus more on tracking the process of heat transfer and mass transfer along with the height of the tower. Reference capacity values that can be used are the value in minimum, equilibrium, and maximum states. The high heat transfer process will be illustrated by high-performance graphics at large capacities.

Nomenclature

The properties of water used in this experiment:

c_{pv}	=	heat capacity of the water vapor
h	=	droplet coefficient of heat transfer
h_{fg}	=	specific enthalpy of evaporation
k_v	=	thermal conductivity of vapor
l_v	=	characteristic length of water vapor
λ_v	=	mean free path of water vapor
μ_v	=	dynamic viscosity of water vapor
v_d	=	kinematic viscosity of water droplet
ρ_l	=	liquid water density
σ	=	surface tension of liquid water
τ_v	=	surface tension of water vapor

References

[1] Chen, G., Zhao, Y., Li, W. & Ge, W., *The Efficiency of High-Level Water Collecting Cooling Tower with The Installation of Cross Wall Affect by The Evolution of Aerodynamic Field*, Applied Thermal Engineering, **161**, 114181, 2019.

[2] Chen, X., Sun, F., Chen, Y. & Gao, M., *Novel Method for Improving the Cooling Performance of Natural Draft Wet Cooling Towers*, Applied Thermal Engineering, **147**, pp. 562-570, 2019.

[3] Chen, X., Sun, F. & Lyu, D., *Field Test Study on Water Droplet Diameter Distribution in The Rain Zone of a Natural Draft Wet Cooling Tower*, Applied Thermal Engineering, **162**, 114252, 2019.

[4] Zunaid, M., Murtaza, Q. & Gautam, S., *Energy and Performance Analysis of Multi Droplets Shower Cooling Tower at Different Inlet Water Temperature for Air Cooling Application*, Applied Thermal Engineering, **121**, pp. 1070-1079, 2017.

[5] Chen, G., Zhao, Y., Ge, W. & Li, W., *Critical Guidelines to Cope with the Adverse Impacts of The Inner Peripheral Vortex in the High-level Water Collecting Natural Draft Wet Cooling Tower*, Applied Thermal Engineering, **168**, 114819, 2020.

[6] Lyu, D., Sun, F. & Zhao, Y., *Experimental Study on the Air Flow Field in the Water Collecting Devices*, Applied Thermal Engineering, **105**, pp. 961-970, 2016.

[7] Wang, M., Wang, J., Wang, J. & Shi, C., *Contrastive Analysis of Cooling Performance between a High-level Water Collecting Cooling Tower and a Typical Cooling Tower*, Journal of Thermal Science, **27**(1), pp. 39-47, 2018.

[8] Fisenko, S.P., Brin, A.A. & Petruchik, A.I., *Evaporative Cooling of Water in A Mechanical Draft Cooling Tower*, International Journal of Heat and Mass Transfer, **47**, pp. 165-177, Jan. 2004.

[9] Chen, L., Huang, X., Yang, L., Du, X. & Yang, Y., *Evaluation of Natural Draft Dry Cooling System Incorporating Water Spray Air Precooling*, Applied Thermal Engineering, **151**, pp. 294-307, 2019.

[10] Fisenko, S.P., Petruchik, A.I. & Solodukhin, A.D., *Evaporative Cooling of Water in a Natural Draft Cooling Tower*, International Journal of Heat and Mass Transfer, **45**(23), pp. 4683-4694, 2002.

[11] Kooij, S., Sijs, R., Denn, M.M., Villermaux, E. & Bonn, D., *What Determines the Drop Size in Sprays?* Physical Review X, **8**, 031019, 2018.

[12] Kuznetsov, G.V., Strizhak, P.A. & Volkov, R.S., *Heat Exchange of an Evaporating Droplet in a High-temperature Environment*, International Journal of Thermal Sciences, **150**, 106227, 2020.

[13] Kuznetsov, G.V., Piskunov, M.V., Volkov, R.S. & Strizhak, P.A., *Unsteady Temperature Fields of Evaporating Water Droplets Exposed to Conductive, Convective and Radiative Heating*, Applied Thermal Engineering, **131**, pp. 340-355, 2018.

[14] Volkov, R.S. & Strizhak, P.A., *Research of Temperature Fields and Convection Velocities in Evaporating Water Droplets Using Planar Laser-Induced Fluorescence and Particle Image Velocimetry*, Experimental Thermal and Fluid Science, **97**, pp. 392-407, 2018.

[15] Movahednejad, E., Ommi, F. & Hosseinalipour, S.M., *Prediction of Droplet Size and Velocity Distribution in Droplet Formation Region of Liquid Spray*, Entropy, **12**, pp. 1484-1498, Jun. 2010.

[16] Minchacam, J.I., Castillejose, A.H. & Acostag, F.A., *Size and Velocity Characteristics of Droplets Generated by Thin Steel Slab Continuous Casting Secondary Cooling Air-Mist Nozzles*, Metallurgical and Materials Transactions B, **42B**, pp. 500-515, 2011.

[17] Afzalifar, A., Saaresti, T.T. & Grönman, A., *Comparison of Moment-Based Methods for Representing Droplet Size Distributions in Supersonic Nucleating Flows of Steam*, Journal of Fluids Engineering, **140**(2), 021301, Sep. 2017.

[18] Onishi, R., Matsuda, K. & Takahashi, K., *Lagrangian Tracking Simulation of Droplet Growth in Turbulence-turbulence Enhancement of Autoconversion Rate*, Journal of the Atmospheric Sciences, **72**, pp. 2591-2607, 2015.

[19] Akkus, Y., Dursunkaya, Z. & Çetin, B., *An Iterative Solution Approach to Coupled Heat and Mass Transfer in a Steadily Fed Evaporating Water Droplet*, Journal of Heat Transfer, **141**(3), 031501, Jan. 2019.

[20] Russo, E., Kuerten, J.G.M., van der Geld, C.W.M. & Geurts, B.J., *Water Droplet Condensation and Evaporation in Turbulent Channel Flow*, Journal of Fluid Mechanics, **749**, pp. 666-700, 2014.

[21] Gilani, N., Hendijani, A.D. & Shirmohammadi, R., *Developing of a Novel Water-Efficient Configuration for Shower Cooling Tower Integrated with the Liquid Desiccant Cooling System*, Applied Thermal Engineering, **154**, pp. 180-195, 2019.

[22] Pedraza, O.J.G., Ibarra, J.J.P., Maya, C.R., González, S.R.G. & Arista, J.A.R., *Numerical Study of the Drift and Evaporation of Water Droplets Cooled Down by a Forced Stream of Air*, Applied Thermal Engineering, **142**, pp. 292-302, 2018.

[23] Strizhak, P.A., Volkov, R.S., Castanet, G., Lemoine, F., Rybdylova, O. & Sazhin, S.S., *Heating and Evaporation of Suspended Water Droplets: Experimental Studies and Modelling*, International Journal of Heat and Mass Transfer, **127**, pp. 92-106, 2018.

[24] Zhao, Y., Sun, F., Long, G., Huang, X., Huang, W. & Lyv, D., *Comparative Study on the Cooling Characteristics of High-level Water Collecting Natural Draft Wet Cooling Tower and the Usual Cooling Tower*, Energy Conversion and Management, **116**, pp. 150-164, 2016.

[25] Li, H.W., Wu, K.B., Wang, S.B., *Numerical Simulation of The Influence of Flue Gas Discharge Patterns on a Natural Draft Wet Cooling Tower with Flue Gas Injection*, Applied Thermal Engineering, **161**, 114137, 2019.

[26] Ni, P., *A Fuel Droplet Vaporization Model in a Hot Air Stream*, Applied Mathematical Modelling, **34**, pp. 2370-2376, 2010.

[27] Huang, X., Chen, L., Yang, L., Du, X. & Yang, Y., *Evaporation Aided Improvement for Cooling Performance of Large-scale Natural Draft Dry Cooling System*, Applied Thermal Engineering, **163**, 114350, 2019.